UFR de mathématique et d'informatique
Université de Strasbourg

cemosis
Centre de modélisation et de simulation de Strasbourg

Eye Kalman Project

Pierre-Antoine Senger

Supervised by: Christophe Prud'homme, Thomas Saigre and Marcela Szopos

August 27, 2025

Overview

1. Context
2. Objectives
3. Laser 101
4. Mathematical Model
5. Discretization
6. Simulations

Context

The Human Eye

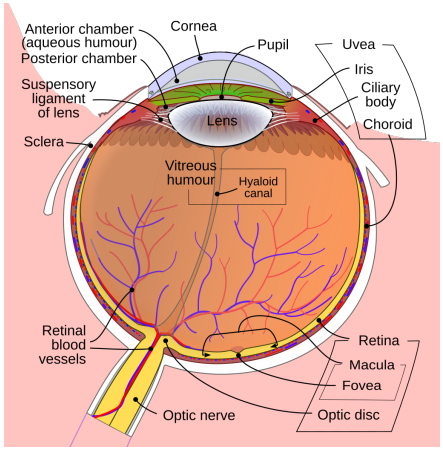

Figure 1: *[Schematic diagram of the human eye. Wikipedia]*

Light-Tissue Interactions

Coefficients of interest: **absorption** $\mu_{a,i}(\lambda)$, **scattering** $\mu_{s,i}(\lambda)$.

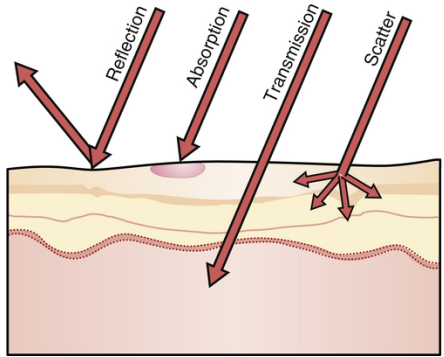

Figure 2: Laser tissue interactions. *["Laser Tissue Interactions: Biological Factors to Consider for Dermatology [Blo19].]*

Objectives

Project Objectives

- **Develop a mathematical model** coupling:
  - **Fluence rate** Φ *[*$\mathrm{W/m^2}$*]*: total radiant power per unit area from all directions.
  - **Temperature** T *[K or* $^\circ\mathrm{C}$*]*: thermal response in tissue.
- Build a realistic **3D geometric model** of the eye.
- Solve the **direct problem**:
  Predict temperature distribution from known optical properties.
- Tackle the **inverse problem** using the Ensemble Kalman Filter (EnKF):
  Estimate tissue optical properties:
  - $\mu_a(\lambda)$: absorption coefficient
  - $\mu_s(\lambda)$: scattering coefficient
- **Visualize** and **analyze** the spatiotemporal results.

Laser 101

Laser Types

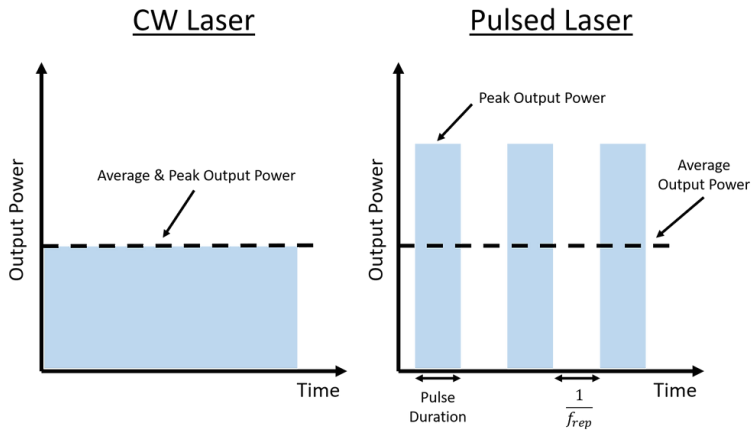

Figure 3: Continuous Wave (CW) vs Pulsed lasers.
[https://www.laser-protect.fr/en/post/laser-operating-modes-continuous-and-pulsed]

Key Parameters

- **Pulse Duration** τ: Ranges from fs (ultrashort) to ms (long-pulse).
- **Wavelength** λ: Distance between wave peaks.
  Optical properties depend on λ: $\mu_a(\lambda)$ = absorption, $\mu_s(\lambda)$ = scattering.
- **Laser Power** P: Typically $0.1\ \mathrm{W}$–$2\ \mathrm{W}$.
- **Beam Waist** w_0: The tightest focus of the beam — where intensity peaks.
- **Beam Divergence** θ: Angular spread of the beam, in rad or mrad. For Gaussian beams:

$$\theta = \frac{\lambda}{\pi w_0}$$

- **Rayleigh Range** z_R: Distance from the waist to where beam cross-section doubles:

$$z_R = \frac{\pi w_0^2}{\lambda}$$

Beam Profiles

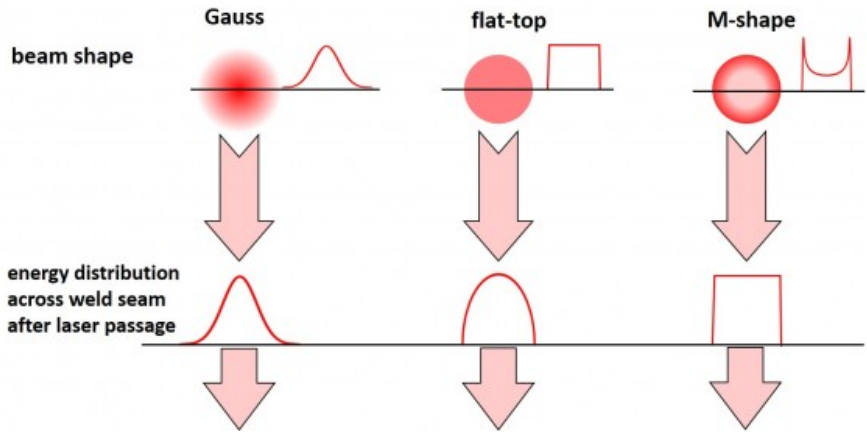

Figure 4: Different beam profiles. *["Beam Profiles" by Probylas]*

Mathematical Model

Eye Geometry $\Omega = \bigcup_{i=1}^{10} \Omega_i$

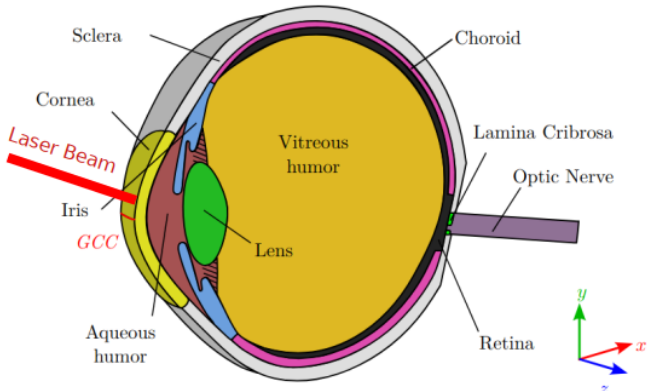

Figure 5: Vertical cut of the geometrical model of the human eye. *["Model order reduction and sensitivity analysis for complex heat transfer simulations inside the human eyeball". Thomas Saigre, Christophe Prud'homme, and Marcela Szopos [SPS24].]*

Eye Geometry: Boundary Conditions

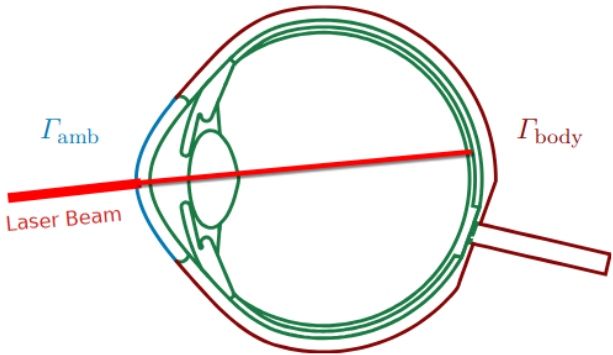

Figure 6: Vertical cut of the geometrical model of the human eye. *["Model order reduction and sensitivity analysis for complex heat transfer simulations inside the human eyeball". Thomas Saigre, Christophe Prud'homme, and Marcela Szopos [SPS24].]*

The Pennes Bioheat Equation

$$
\begin{cases}
\rho_i C_{p_i} \dfrac{\partial T_i}{\partial t} - \nabla \cdot (k_i \nabla T_i) = Q_{\mathrm{l},i} + Q_{\mathrm{m},i} + Q_{\mathrm{p},i} & \text{on } \Omega = \displaystyle\bigcup_{i=1}^{10} \Omega_i, \\
-k_i \nabla T_i \cdot n_i = \underbrace{h_{\mathrm{amb}}(T_i - T_{\mathrm{amb}})}_{(i)} + \underbrace{\sigma \varepsilon (T_i^4 - T_{\mathrm{amb}}^4)}_{(ii)} + \underbrace{E}_{(iii)} & \text{on } \Gamma_{\mathrm{amb}}, \\
-k_i \nabla T_i \cdot n_i = h_{\mathrm{bl}}(T_i - T_{\mathrm{bl}}) & \text{on } \Gamma_{\mathrm{body}}, \\
T_i = T_j & \text{on } \Omega_i \cap \Omega_j, \\
k_i \nabla T_i \cdot n_i = -k_j \nabla T_j \cdot n_j & \text{on } \Omega_i \cap \Omega_j.
\end{cases}
$$

$Q_{\mathrm{l},i} = \mu_{a,i}(\lambda) \times \Phi_\lambda(x, y, z)$: **laser** heat generation,

$Q_{\mathrm{m},i}$: **metabolic** heat generation $\rightarrow$ ignored since negligible compared to the others,

$Q_{\mathrm{p},i} = \rho_{\mathrm{bl}} \omega_{\mathrm{bl}} C_{p_{\mathrm{bl}}} (T_{\mathrm{bl}} - T_i)$: blood **perfusion** heat generation.

The Radiative Transfer Equation (RTE)

Describes the propagation of light in a medium.

$$\left(\frac{1}{c}\frac{\partial}{\partial t} + s \cdot \nabla + \mu_a(r) + \mu_s(r)\right) L(r, s, t) = \mu_s(r) \int_{4\pi} L(r, s', t)\beta(s, s')\mathrm{d}s' + Q(r, s, t),$$

$L(r, s, t)$: **radiance** at position r, in direction s, $(r, s) \in \mathbb{R}^3 \times \mathbb{S}^2$
c: speed of light $[\mathrm{ms}^{-1}]$,
$\beta(s, s')$: phase function [dimensionless].

$s \cdot \nabla$: **advection** — directional transport of light,
$\mu_a(r) + \mu_s(r)$: **attenuation** due to absorption and scattering,
$\mu_s(r) \int \cdots$: **in-scattering** contribution,
$Q(r, s, t)$: **source** term.

The Diffusion Approximation

Valid when $\mu_a \ll \mu_s$.

$$\begin{cases} \dfrac{1}{c}\dfrac{\partial \Phi_i}{\partial t} - \nabla \cdot \left(D_i \nabla \Phi_i\right) + \mu_{a,i}(\lambda)\Phi_i = S & \text{on } \Omega = \bigcup_{i=1}^{10} \Omega_i, \\ \Phi_i + 2\,\alpha_i D_i \nabla \Phi_i \cdot n_i = \Phi_{\text{amb}} & \text{on } \Gamma_{\text{amb}}, \\ \Phi_i + 2\,\alpha_i D_i \nabla \Phi_i \cdot n_i = 0 & \text{on } \Gamma_{\text{body}}, \\ \Phi_i = \Phi_j & \text{on } \Omega_i \cap \Omega_j. \end{cases}$$

$D_i = \dfrac{1}{3\left(\mu_{a,i}(\lambda) + \mu'_{s,i}(\lambda)\right)}$: diffusion coefficient,

$\alpha_i = \dfrac{1+R_i}{1-R_i} \in [0,1]$: albedo (*i.e.* fraction of light scattered back),

R_i: reflection coefficient.

The MC Approach (RTE-MC)

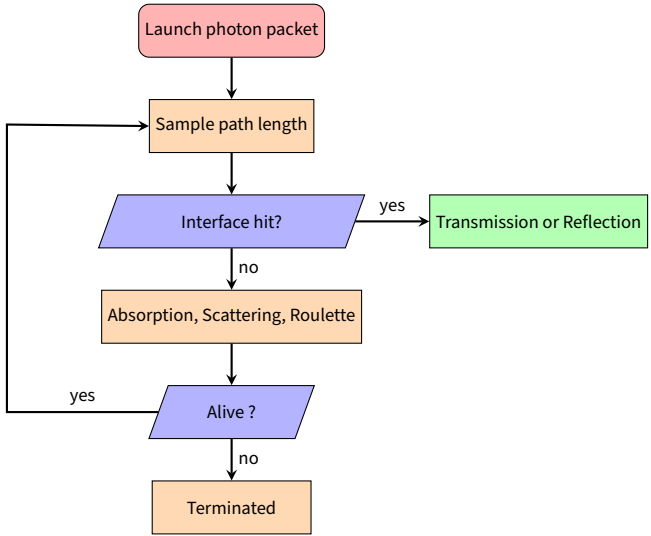

RTE-MC: Beer-Lambert Law

Using the **Beer-Lambert law**, for a **homogeneous medium** of length x we have:

$$N_x = N_0 \, e^{-\mu_t x}$$

Where:

- $\mathbf{N_0}$: initial number of photons
- $\mathbf{N_x}$: number of photons after traveling distance x
- $\mu_\mathbf{t} = \mu_\mathbf{a} + \mu_\mathbf{s}$: attenuation coefficient, sum of absorption μ_a and scattering μ_s

RTE-MC: Path Length Distribution

The probability density function (PDF) of the photon path length x in a medium is:

$$f_x(x) = \underbrace{\mu_t}_{\text{attenuation coeff.}} e^{-\mu_t x} \mathbb{1}_{\{x \geq 0\}}$$

The cumulative distribution function (CDF) is given by:

$$F_x(x) = \int_{-\infty}^{x} f_x(t)dt = \int_0^x \mu_t e^{-\mu_t t} dt$$

Evaluating the integral:

$$F_x(x) = \mu_t \left[-\frac{1}{\mu_t} e^{-\mu_t t} \right]_0^x = 1 - e^{-\mu_t x} \mathbb{1}_{\{x \geq 0\}}$$

Note: $F_x(x)$ is strictly increasing on $\mathbb{R}^+$ and hence invertible, allowing us to sample path lengths from uniform random variables.

RTE-MC: Inverse Transform Sampling

We want to find the **inverse** of the CDF to sample path length x from a uniform random variable $\xi \sim U(0,1)$.

$$
\begin{aligned}
y &= 1 - e^{-\mu_t x}, \quad y \in (0,1) \\
e^{-\mu_t x} &= 1 - y \\
-\mu_t x &= \ln(1-y)
\end{aligned}
$$

Since $y \in (0,1)$, define $\xi := 1 - y \in (0,1)$. Then

$$
s := x = -\frac{\ln(\xi)}{\mu_t}
$$

RTE-MC: Anisotropic Scattering

When the medium is **anisotropic**, the photon travels a distance s in a random direction θ and then scatters.

To sample the **scattering angle** θ, we use the **Henyey-Greenstein** phase function:

$$\cos(\theta) = \begin{cases} 2\xi - 1 & \text{if } g \approx 0 \\ \dfrac{1 + g^2 - \left(\frac{1-g^2}{1-g+2g\xi}\right)^2}{2g} & \text{otherwise} \end{cases}$$

Here, $g \in (-1, 1)$ is the **anisotropy factor**, representing the degree of forward scattering.

RTE-MC: Energy Deposition

At each space step s, the photon (or photon packet) deposits part of its **energy** w (initialized at 1) into the element it lands in.

$$w \leftarrow w \cdot \frac{\mu_a}{\mu_t}$$

Where w is the updated energy of the photon packet after absorption in the current element.

Note: Intermediate elements traversed between steps may not receive any energy deposition unless explicitly handled.

RTE-MC: Absorption Map

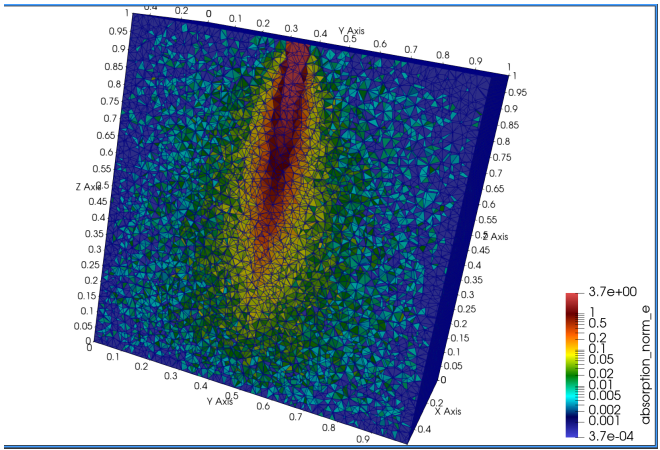

Figure 7: Early results of the map of absorption on a cube.

Bounding Volume Hierarchy (BVH)

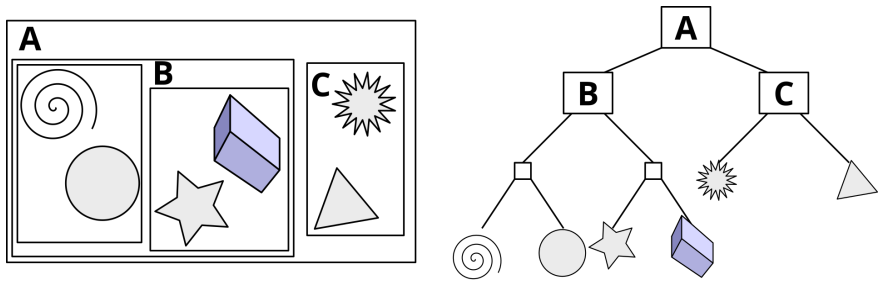

Figure 8: Example of bounding volume hierarchy (BVH) in two dimensions. *[Wikipedia]*

RTE-MC: Fresnel Illustration

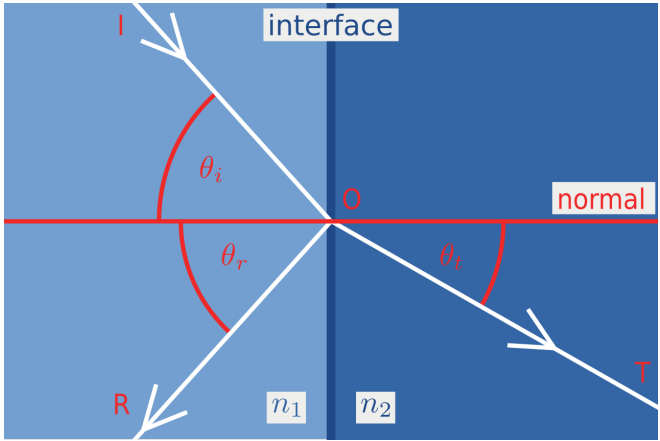

Figure 9: Fresnel equations illustrated ($\theta_i = \theta_r$). *["Fresnel equations" Wikipedia]*

RTE-MC: Interface Interactions

When a photon hits an interface Ω_{ij}:

- **Snell's law** gives the refracted direction:

$$\boxed{n_1 \sin(\theta_i) = n_2 \sin(\theta_t)}$$

- **Fresnel equations** (or Schlick's approximation) give the reflection probability:

$$\boxed{R(\theta_i) \approx R_0 + (1 - R_0)(1 - \cos\theta_i)^5}$$

with $R_0 = \left(\frac{n_1 - n_2}{n_1 + n_2}\right)^2$.

Algorithm:

- Draw $u \sim \mathcal{U}(0, 1)$.
- If $u < R(\theta_i)$: reflect, else refract.

RTE-MC: Russian Roulette

We expect the photon's energy to decrease rapidly. To avoid tracking all low-energy photons while maintaining physical accuracy, we use the **Russian Roulette** technique. Let $p \in (0, 1)$ be the survival probability. If $w < w_{\text{min}}$, then:

Russian Roulette:
Sample a realisation $\xi \sim \mathcal{U}(0, 1)$
if $\xi < p$ **then**
    Photon survives: $w \leftarrow \frac{w}{p}$
else
    Photon is terminated
end if

Pennes Bioheat Equation & RTE-MC Coupling

- The RTE-MC provides the **normalized absorption map A**.
- The source term Q_l in the **Pennes equation** is given by:

$$\boxed{Q_l(x, y, z) = P \times A}$$

  where P is the **laser power** and A is the **absorption map** from RTE-MC.
- Solving the **Pennes equation** yields the temperature distribution $T(x, y, z)$ within the eye.

This coupling allows simulation of light-induced heating effects with spatial precision.

Discretization

Space Discretization

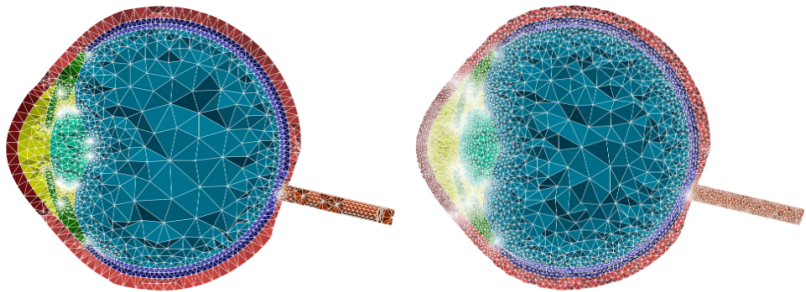

(a) Original mesh generated by Salome, with $4.64 \cdot 10^5$ tetrahedrons: $h_{\min} = 5.77 \cdot 10^{-6}, h_{\max} = 5.76 \cdot 10^{-3}$.

(b) Mesh refined around the anterior and posterior chambers, with $9.4 \cdot 10^5$ elements: $h_{\min} = 5.09 \cdot 10^{-5}, h_{\max} = 3.12 \cdot 10^{-3}$.

Figure 10: Meshed geometry of the eye, over a vertical plane. Characteristic sizes are given in meters. *["Model order reduction and sensitivity analysis for complex heat transfer simulations inside the human eyeball". Thomas Saigre, Christophe Prud'homme, and Marcela Szopos [SPS24].]*

Space Discretization: Test Case

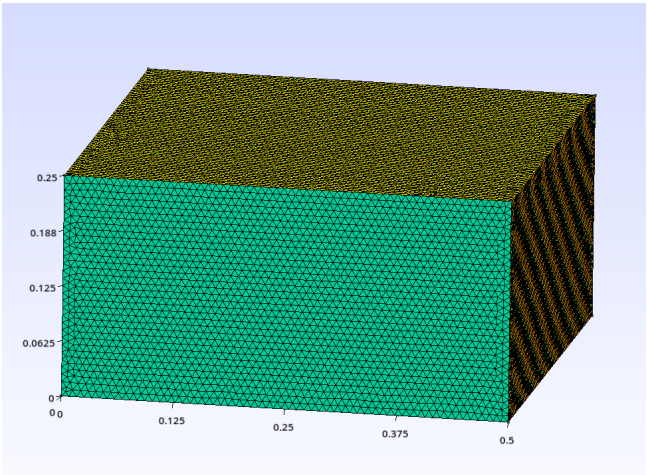

Figure 11: 0.5 x 0.5 x 0.25 cm single layer cube with 81907 nodes and 495013 elements.

Simulations

RTE-MC Simulation Parameters

- **Beam Diameter**: 0.2 cm
- **Absorption Coefficient** μ_a: 5 cm^{-1}
- **Scattering Coefficient** μ_s: 100 cm^{-1}
- **Anisotropy Factor** g: 0.9
- **Number of Photons**: 2,000,000

RTE-MC: Absorption Map

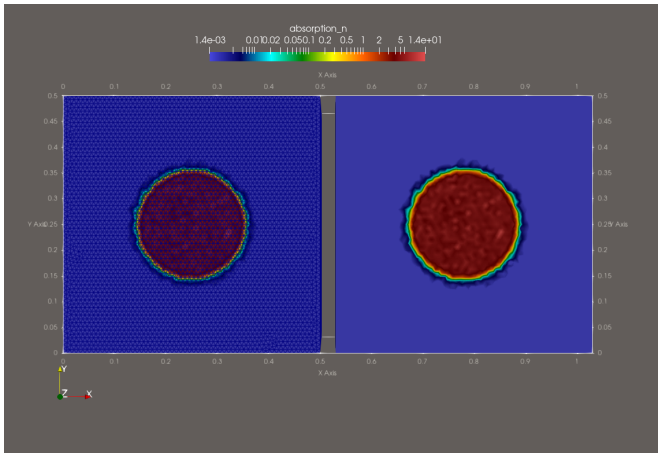

Figure 12: Log scale top view of the absorption map.

RTE-MC: Absorption Map

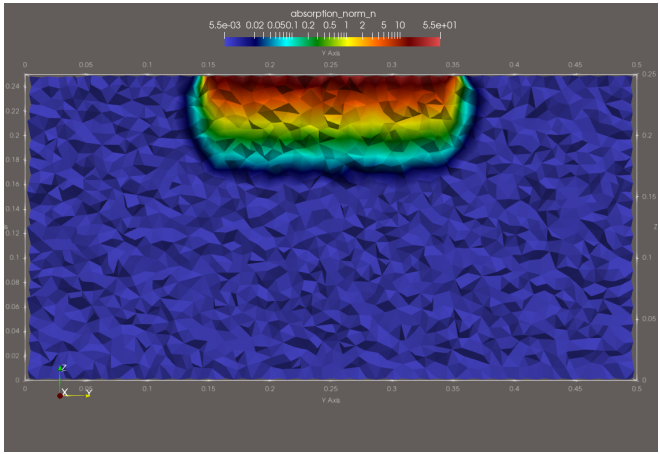

Figure 13: Log scale clipped view of the absorption map for the cube geometry.

Heat Simulation Parameters

- **Laser Power** P: 0.5 W
- **Simulation Time Step** Δt: 0.01 s
- **Total Simulation Time** T: 15 s
- **Time Scheme**: Crank-Nicolson
- **Boundary Conditions**: Homogeneous, Neumann on top, Dirichlet on others
- **Initial Temperature** T_0: 0 °C

Heat Simulation Results

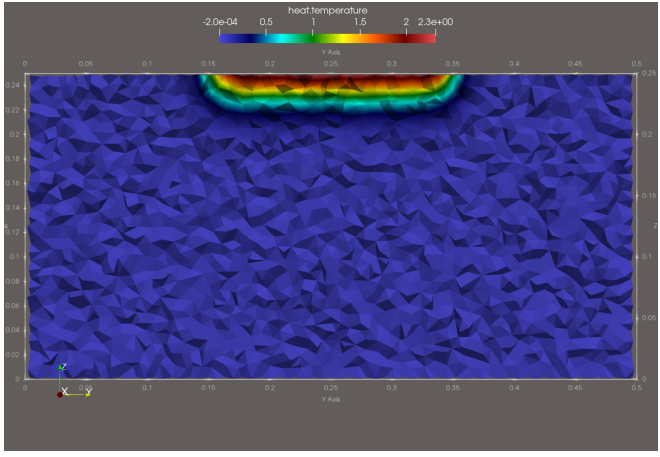

Figure 14: t=0.2 s

Heat Simulation Results

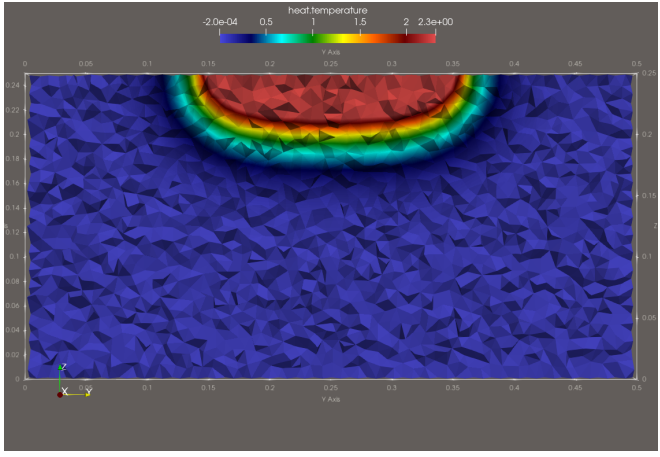

Figure 15: t=1 s

Heat Simulation Results

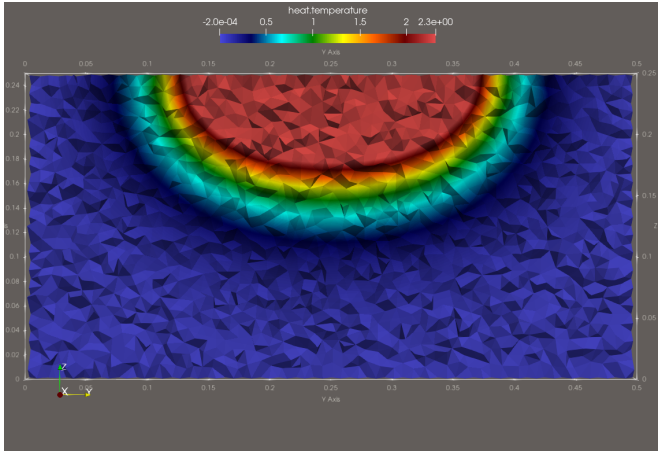

Figure 16: t=3 s

Heat Simulation Results

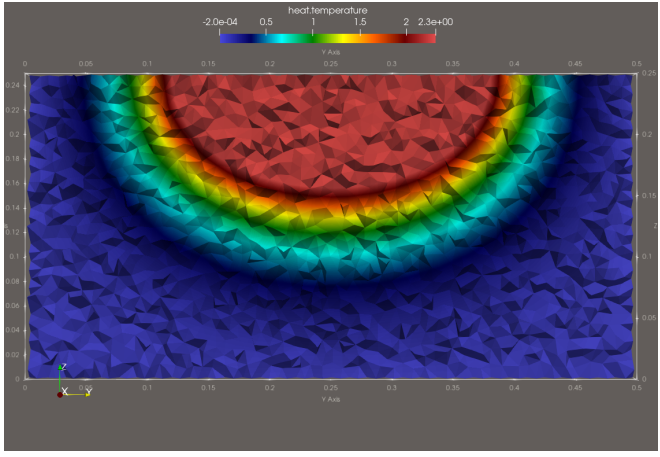

Figure 17: t=5 s

Heat Simulation Results

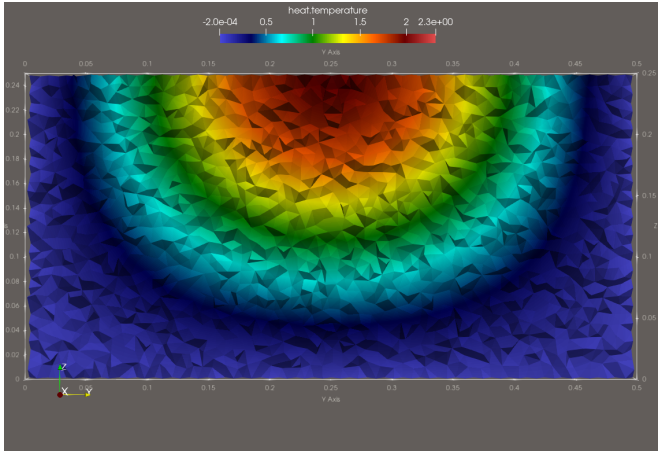

Figure 18: t=10 s

Heat Simulation Results

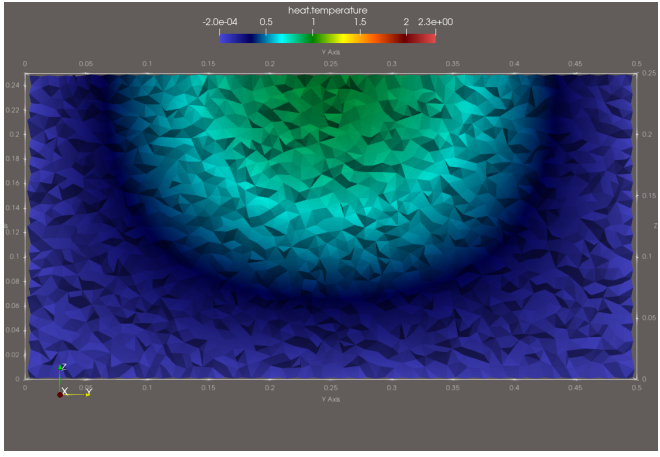

Figure 19: t=15 s

The end

Thank you for your attention!

Any questions?

Contact Information:

`pierre.antoine.senger@gmail.com`

`github.com/pa-senger`

References

[Blo19] FindLight Blog. *Laser Tissue Interactions: Biological Factors to Consider for Dermatology*. 2019. URL: https://www.findlight.net/blog/laser-tissue-interactions/.

[SPS24] Thomas Saigre, Christophe Prud'homme, and Marcela Szopos. "Model Order Reduction and Sensitivity Analysis for Complex Heat Transfer Simulations inside the Human Eyeball". In: *International Journal for Numerical Methods in Biomedical Engineering* 40.11 (Sept. 9, 2024), e3864. ISSN: 2040-7939, 2040-7947. DOI: 10.1002/cnm.3864. URL: https://onlinelibrary.wiley.com/doi/10.1002/cnm.3864.

Heat Simulation Validation

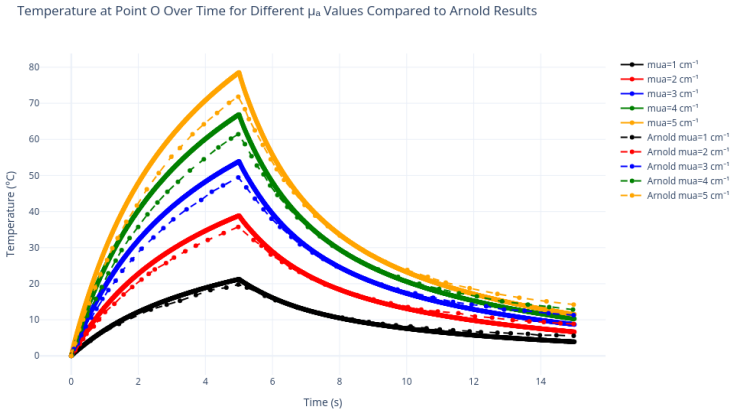

Figure 20: Validation of heat simulation results.

Heat Simulation Validation

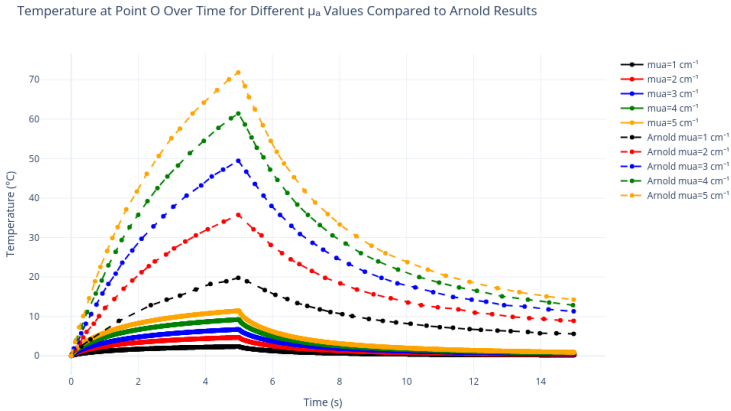

Figure 21: New algo results vs Arnold.